*ORIGINAL PAPER*

# STRUCTURAL HARDENING MECHANISM OF THE NICKEL-BASED ALLOY "HASTELLOY G30"

O. BEN LENDA[1], F. SABIR[1], S. SAISSI[1], A. IBNLFASSI[1], Y.TAMRAOUI[2], F. MIRINIOUI[2], L. ZERROUK[1], B.MANOUN[2], E. SAAD[1]

*Manuscript received: 03.04.2015; Accepted paper: 17.05.2015; Published online: 30.06.2015.*

***Abstract.*** *The superalloy Hastelloy G30 (trademark of Haynes International, Inc.) is an alloy with a high proportion of nickel, characterized by a high corrosion resistance in environments containing extra oxidizing acids. The alloy consists essentially of 43% of nickel with a proportion of chromium which varies from 28 to 31.5% and from 13 to 17% for iron. Its matrix is austenitic and its structure is face-centered cubic.*

*The objective of this work is to treat the alloy G30 thermally at 4 different temperatures 700 °C, 800 °C, 900 °C and 1000 °C for 3 hours. Indeed, we followed the progression of structural and mechanical properties.*

*The micro structural evolution influence slightly on the mechanical properties of the alloy G30: hardness of the alloys treated at 700 °C and 800 °C is equal to 46 HRF and that of the alloys treated at 900 °C and 1000 °C is 46.25 HRF. The images obtained by optical microscopy revealed the presence of carbides at the joints and inside the grains .The X-ray diffraction spectra obtained after the isothermal treatments showed the presence of peaks of the precipitates and the peaks of the austenite phase.*

***Keywords:*** *aging, alloys, carbide, thermal treatments, hardness, optical microscopy, X-ray diffraction.*

## 1. INTRODUCTION

The large family of nickel-based alloys has been empirically developed over the last 60 years from a matrix consisting of nickel-chromium [1]. These austenitic alloys have a face-centered cubic structure which mechanical properties are improved compared to alloys with centered cubic structure [1].

Maintaining the percentage of chromium between 20% and 33%, molybdenum between 1.5% and 7% and by replacing the nickel with iron to reduce their price allowed given alloys resistant to corrosive reducers acids [2]. The corrosion resistance mechanism

at high temperature in a corrosive environment is based on the formation of a protective chromium layer $Cr_2O_3$ [3].

The austenitic nickel matrix hardens by the addition of cobalt, iron, chromium, molybdenum and tungsten. Nickel has a high solubility with iron and can melt with almost 35% by weight chromium, 20% for each of molybdenum and tungsten and from 5% to 10% of manganese [4].

Resistance to the aggressiveness of the environment while keeping its chemical stability is a challenge for these alloys because they are used in the nitric acid Service, the

[1] Université Hassan 1er FST Settat, Laboratoire Physico-Chimie des Procédés et des Matériaux(PCPM), Maroc. E-mail: saadelmadani73@gmail.com.
[2] Université Hassan 1er, Laboratoire des Sciences des Matériaux, des Milieux et de la modélisation (LS3M), Maroc.

phosphoric acid service, petrochemical applications [2] etc. However, at a high temperature, the carbon diffuses into the matrix which promotes the formation of carbides. Therefore, changes occur in mechanical and chemical properties. For example, the formation of chromium carbides in the grain boundaries depletes zones close to grain boundaries of chromium which leads to corrosion [5].

The aim of this work is to study the influence of heat treatment on the structural and mechanical behavior of the nickel-based alloy G30.

## 2. MATERIALS AND METHODS

### *2.1. PREPARATION OF ALLOYS*

A plate is supplied by the HAYNES International, Inc company. The samples, obtained by sawing, have a square shape of dimensions 20 mm × 19.5 mm and thickness of to 3 mm. The composition of the alloy G30 which was the subject of the metallurgical study is given in the table 1 below:

**Table 1. Chemical composition of the alloy G30.**

| Ni[a] | Co | Cr | Mo | W | Fe | Si | Mn | C | others |
|---|---|---|---|---|---|---|---|---|---|
| 43 | 5.0 ** | 28.0 - 31.5 | 4.0 - 6.0 | 1.5 - 4.0 | 13.0 - 17.0 | 0.8 ** | 1.5 ** | 0.03 ** | Cb + Ta = 0.3-1.5<br>Cu = 1.0-2.4<br>P = 0.04 **<br>S = 0.02 ** |

** Maximum Percentage, a: Balance.

According to ternary phase diagrams Ni-Cr-Fe [6], Nickel as a majority component with a content of 28 to 31% of chromium and 13 to 17% of iron, the alloy is austenitic at different temperatures of treatments. We observe also that by increasing the temperature and the concentration of nickel the austenitic domain widens while chromium tends to favor crystallization of alpha phase.

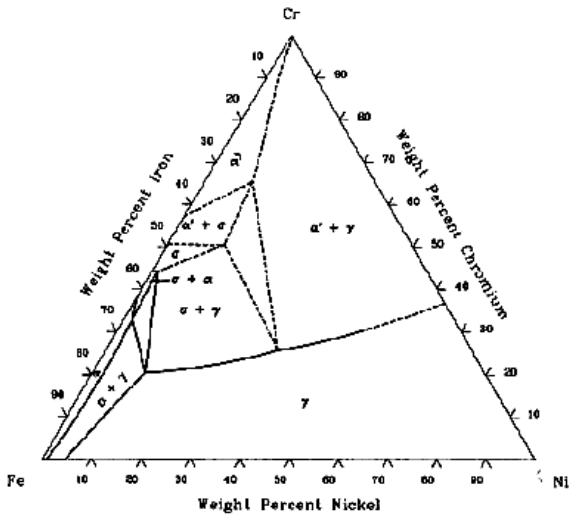


**Figure 1. Phase diagram Ni-Cr-**Fe **at 650 ° C.**

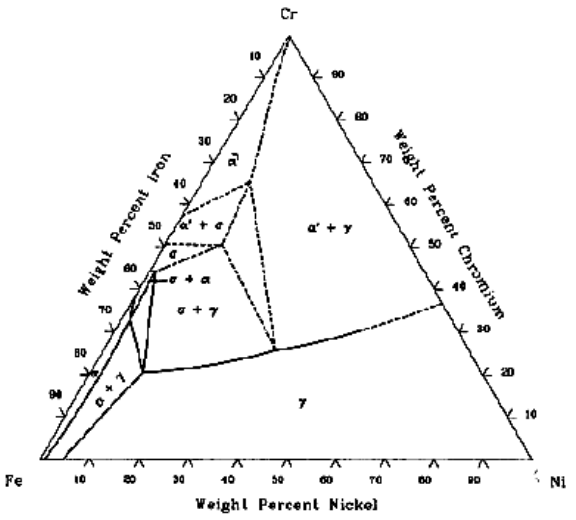


**Figure 2. Phase diagram Ni-Cr-**Fe **at 800 °**

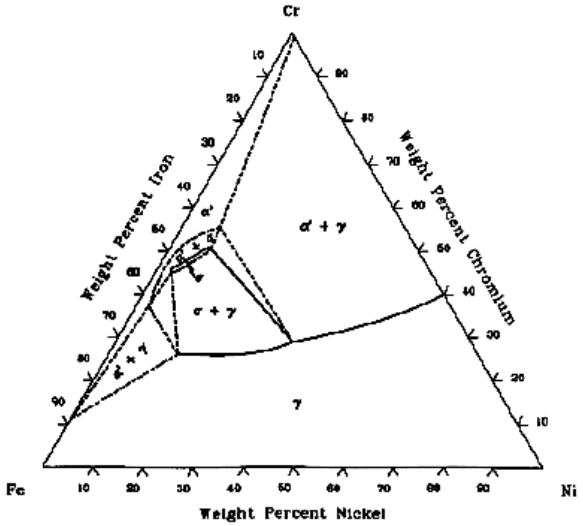


**Figure 3. Phase diagram Ni-Cr-Fe at 900 ° C.**

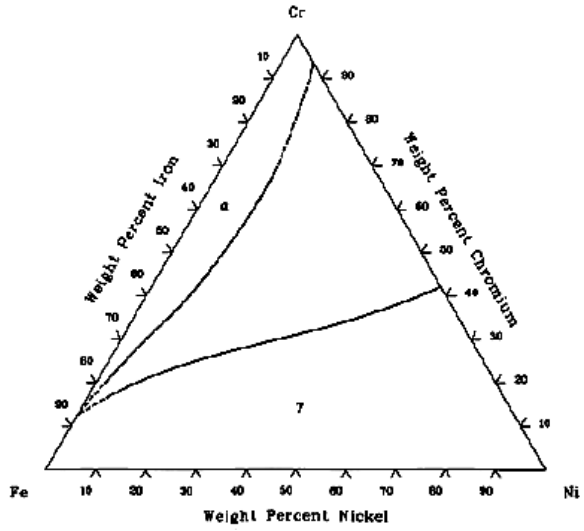


**Figure 4. Phase diagram Ni-Cr-Fe at 1000 ° C.**

*2.2. HARDNESS*

Hardness tests are performed using a universal Durometer according to the method of ROCKWELLF (HRF): The indenter used is steel ball type 1.588 mm in diameter under a load of 60 kgf. Each measurement is the average of 5 marks well distributed on the flat section. These sections are obtained by polishing and finishing using abrasives turning around a fixed axis with water lubrication to avoid overheating which could cause changes in structure.

*2.3. X-RAY DIFFRACTION*

The X-ray diffraction spectra of the four samples during aging and over-aging are obtained at room temperature using D2 PHASER diffractometer, Bragg-Brentano geometry, radiation type Cu Kα = 1.5406 Å and the scanning interval is 15 to 100 ° with a step of 0.01 (2θ).

*2.4. OPTICAL MICROSCOPY*

By increasing temperature, diffusion of carbon increases and tends to form carbides with some metallic elements which affect the structure of the alloys. In order to detect changes in structure, we used optical microscopy. In general, Micrographic observation requires physical polishing and chemical etching. In the case of nickel-based alloys, chemical etching is performed by aqua regia used immediately after preparation. The etching solution reveals grain boundaries and carbides, and it consisting of HCl and HNO3 of with a proportion of 3: 1 and immersion time between 5 and 60 seconds [7].

## 3. RESULTS AND DISCUSSION

*3.1. THE STUDY OF THE ALLOY G30 TREATED AT T = 800 ° C*

*3.1.1. Hardness measurement*

According to Fig. 5, the hardness increases from 47.33 HRF to 49HRF in 170 minutes then remains almost constant until 20 hours (49.25 HRF). After, we notice a remarkable increase to reach maximum hardness of 52.17 HRF in 4 days. Then it decreases to reach a

value of 46 HRF after 44 days. The hardness curve in Fig. 5 shows that the aging kinetic is slow unlike overaging where the kinetic is fast.

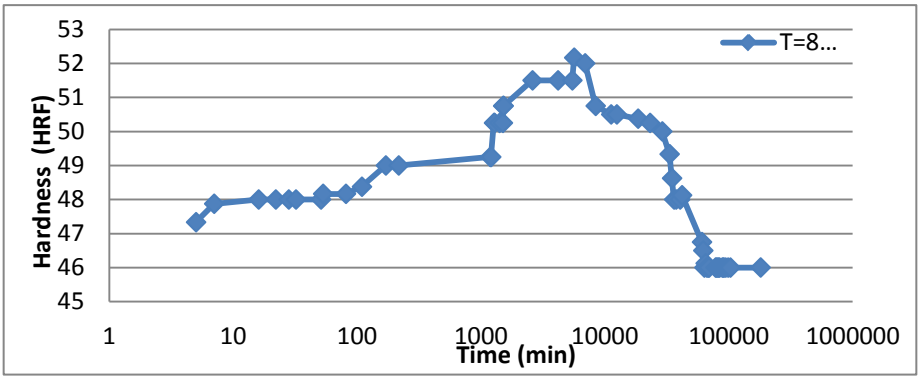


**Figure 5. Evolution of hardness in HRF of piece treated at 800°C as function of time**

*3.1.2. OPTICAL MICROSCOPY*

The figures show that the precipitation is intergranular and intragranular with different morphologies. Fig. 6 shows a precipitation of carbides at grain boundaries γ/γ after 45 minutes of quenching, which constitutes privileged sites for precipitation [8]. The grain boundaries have a high interfacial energy [9] and they are considered as preferential site for precipitation which propagates after, inside the grains. They form a continuous "film" on grain boundaries that leads to degradation of mechanical properties [3]. In Fig. 7, we note after 50 minutes of quenching the apparition of dendritic morphology formed when the cooling rate is very high.

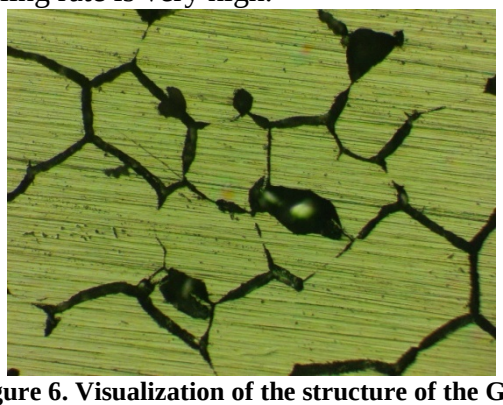

**Figure 6. Visualization of the structure of the G30 alloy treated at 800°C, attacked with aqua regia, after 45 min of quenching**

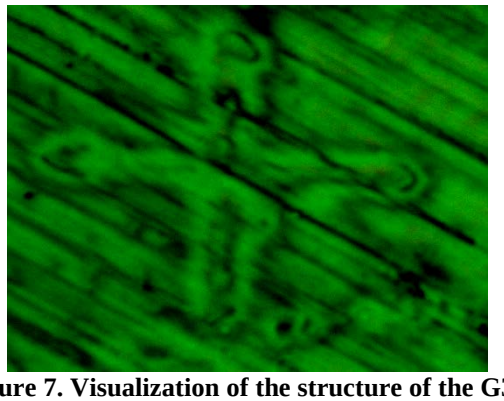

**Figure 7. Visualization of the structure of the G30 alloy treated at 800°C, attacked with aqua regia, after 50 min of quenching.**

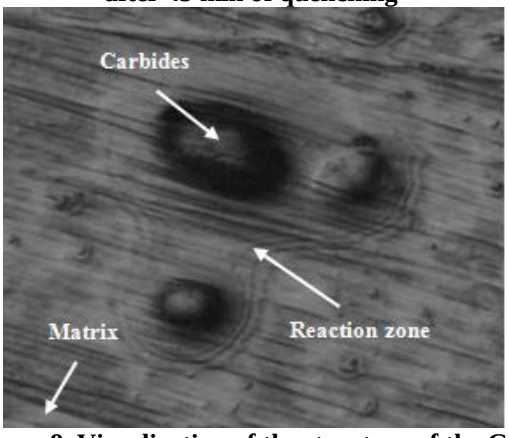


**Figure 8. Visualization of the structure of the G30 alloy treated at 800°C, attacked with aqua regia, after 70 days of quenching.**

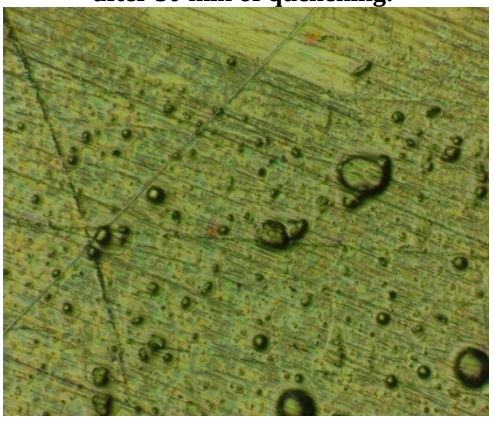

**Figure 9. Visualization of the structure of the G30 alloy treated at 800°C, attacked with aqua regia, after 70 days of quenching**

Fig. 8 shows the appearance of carbides of granular form after 70 days of quenching which they are often secondary carbides resulting from the decomposition of intergranular carbides. The evolution of hardness of the alloy is intimately linked to movements of fronts of carbides. Also, we notice on the same figure, the coalescence phenomenon that leads to increase the size of carbides. Fig. 9 shows that after overaging (70 days) the matrix of the alloy is covered with large areas of precipitates which leads to the decrease of hardness.

### *3.1.3. X-RAY DIFFRACTION*

We remark that the structure is homogeneous and remains austenitic, characterized by planes (110), (200), (220), (311) and (222). We also note the appearance of a new peak after treatment at position $2\theta \simeq 28,15°$ due to the formation of carbides in the matrix. Based on ASTM specifications, the positions (b), (c) and (d) correspond to peaks consisting of doublets relative to matrix and carbides confirmed by images obtained by optical microscope.

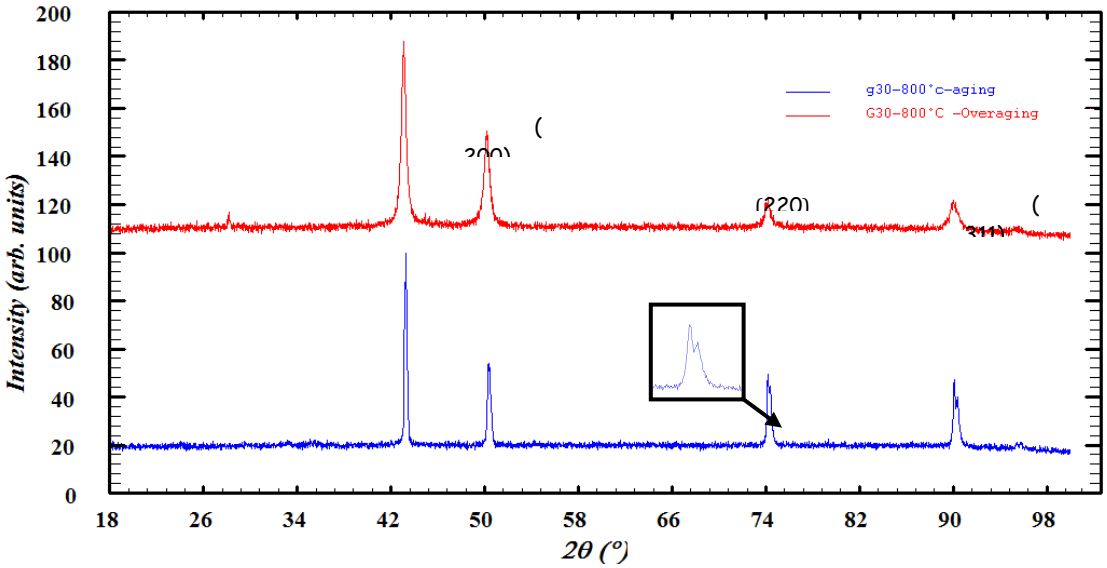


**Figure 10. X-ray diffraction spectra of the alloy G30 during aging and over-aging treated at 800°C.**

### *3.2. THE STUDY OF THE INFLUENCE OF THE THERMAL TREATMENT*

#### *3.2.1. Hardness measurement*

As shows fig. 11, The temperature affects aging duration, that lasts for 18,53 hours (51.25 HRF) at 700°C , 4 days (52.17 HRF) at 800°C, 20 hours (52.25 HRF) at 900°C and finally 118 minutes (51.5 HRF) at 1000°C. The temperature act slightly on the final mechanical properties of the alloy G30: the final hardness of alloys treated at 700 ° C and 800 ° C is equal to 46 HRF and for the alloys treated at 900 ° C and 1000 ° C is 46.25HRF.

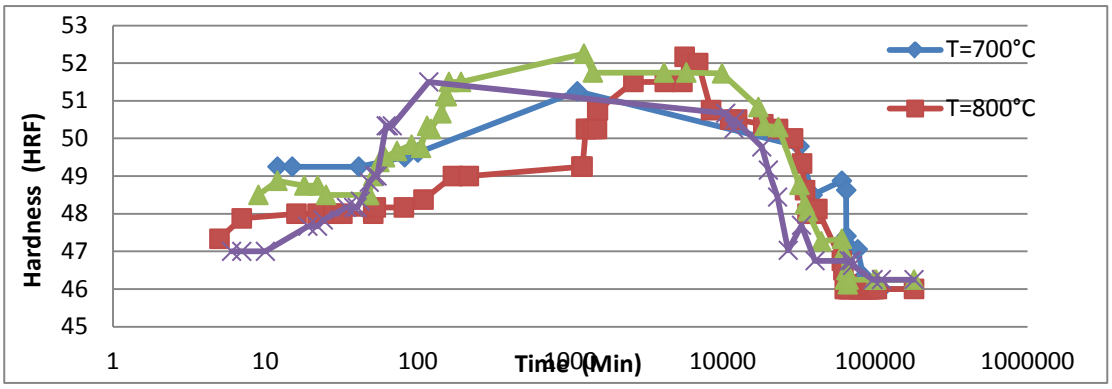


**Figure 11. The evolution of the hardness of the piece treated at 700°C, 800°C, 900°C and 1000°C as function of time**

- For temperature 700 ° C, hardness increases progressively and reaches a maximum value of 51.25 HRF after 19 hours. After, it decreases with a very slow kinetics to achieve final hardness of 46 HRF after 60 days.
- For temperature 900°C, there is a preliminary phase of rapid and important hardening from 48.5 to 51.5 HRF after 3 hours, followed by a progressive hardening in function of time to reach a maximum value of 52.25HRF after 20 hours then a slight decrease of hardness during over-aging to the value 46.46 HRF after 46 days.
- For temperature 1000°C, the aging phase is reached quickly just after 118 minutes (51.5 HRF) followed by a slight decrease of hardness before stabilizing at 46.25HRF after 67 days.

*3.2.2. OPTICAL MICROSCOPY*

The figs 12-17 show a dispersion of fine precipitates in matrix and the presence of carbides at grain boundaries during aging for the different temperatures 700°C, 900°C and 1000°C. We observe for temperature 1000°C, in figure 18, the appearance of lamellar morphology which they are eutectic precipitates constituted by carbides and austenite.

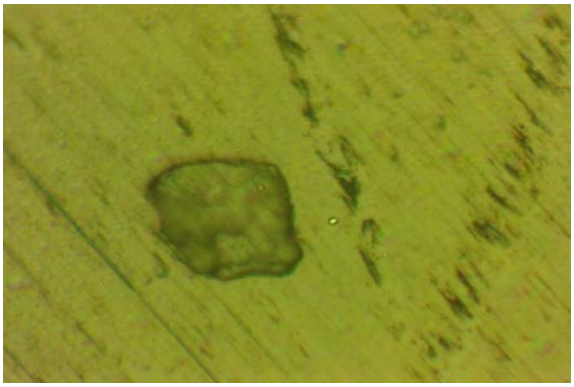

**Figure 12. Visualization of the structure of the G30 alloy treated at 700°C, attacked with aqua regia, after 21 hours from quenching**

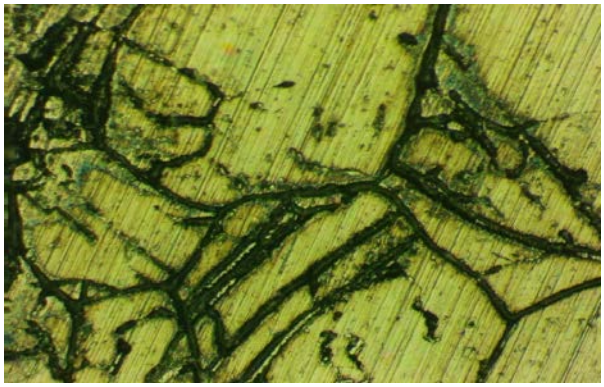

**Figure 13: Visualization of the structure of the G30 alloy treated at 700°C, attacked with aqua regia, after 74 min from quenching**

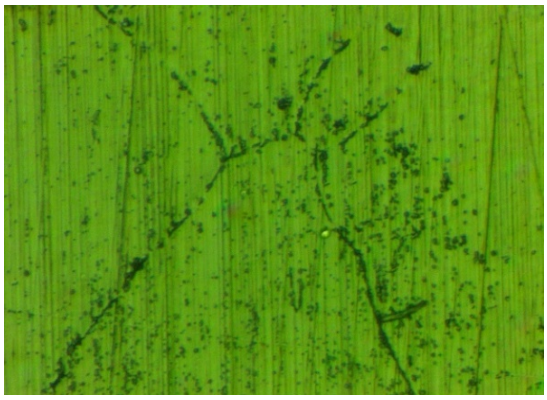

**Figure 14. Visualization of the structure of the G30 alloy treated at 900°C, attacked with aqua regia, after 108 min from quenching.**

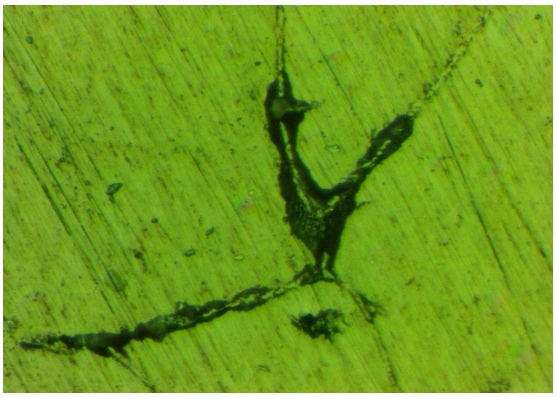

**Figure 15. Visualization of the structure of the G30 alloy treated at 900°C, attacked with aqua regia, after 82 min from quenching.**

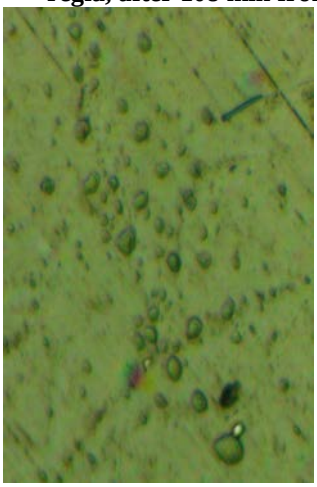

**Figure 16. Visualization of the structure of the G30 alloy treated at 1000°C, attacked with aqua regia, after 35 min from quenching**

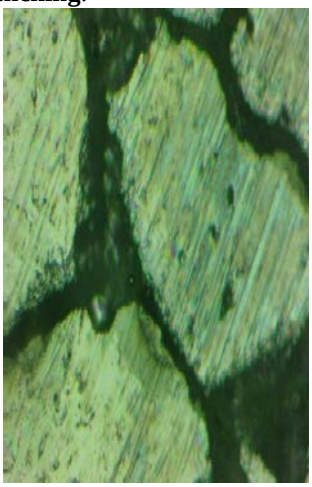

**Figure 17. Visualization of the structure of the G30 alloy treated at 1000°C, attacked with aqua regia, after 96 min from quenching**

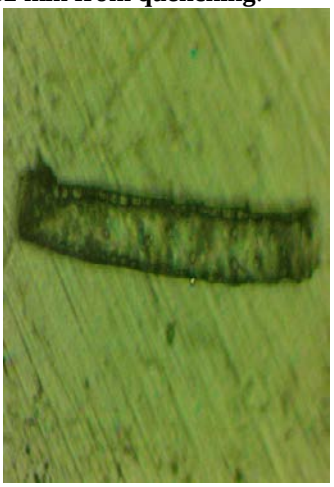

**Figure 18. Visualization of the structure of the G30 alloy treated at 1000°C, attacked with aqua regia, after 54 min from quenching**

**Figure 19. Visualization of the structure of the G30 alloy treated at 700°C, attacked with aqua regia, after 68 days from quenching.**

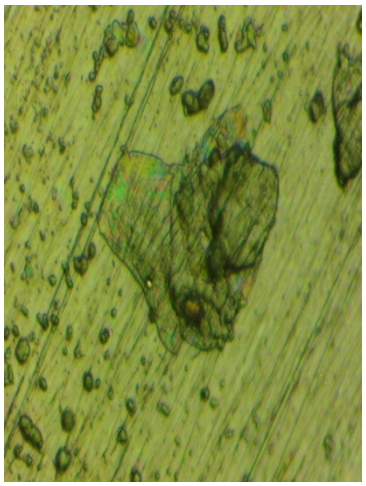

**Figure 20. Visualization of the structure of the G30 alloy treated at 900°C, attacked with aqua regia, after 69 days from quenching**

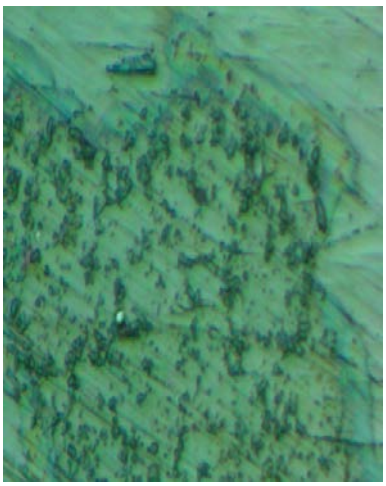

**Figure 21. Visualization of the structure of the G30 alloy treated at 1000°C, attacked with aqua regia, after 53 days from quenching**

The figs. 19-21 correspond to thermal treatments 700°C, 900°C and 1000°C. We remark that the resulting matrix of samples during overaging for different temperatures is covered by large areas of precipitates.

*3.2.3. X-RAY DIFFRACTION*

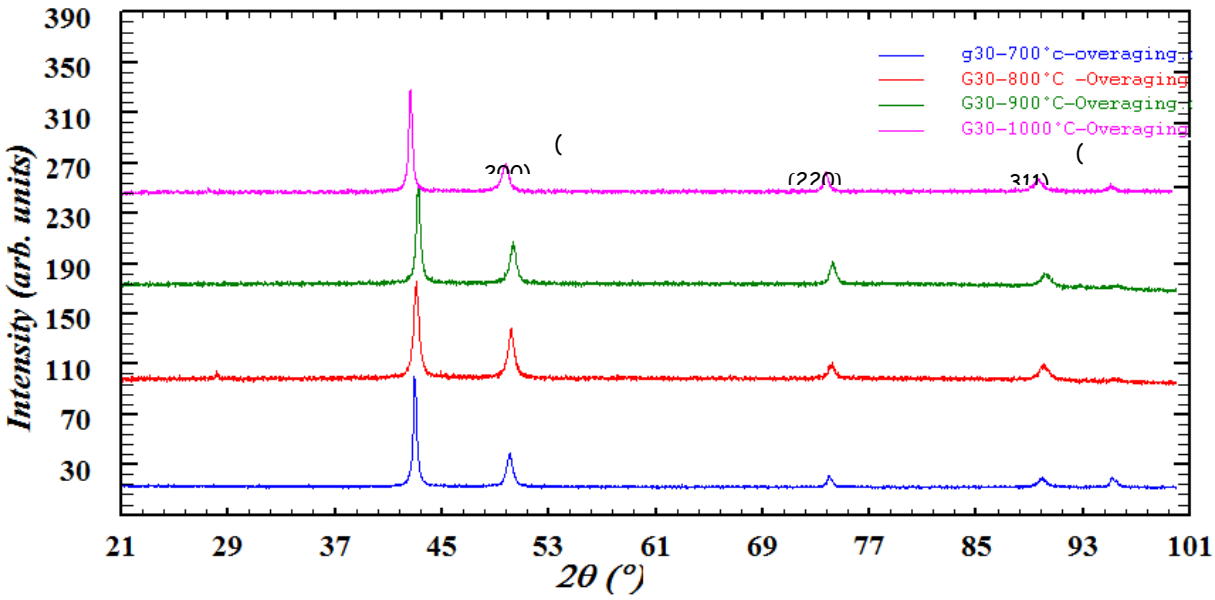


**Figure 22. X-ray diffraction spectra of the G30 alloy treated at 700 ° C, 800 ° C, 900 ° C and 1000 ° C during overaging**

Fig. 22 shows that the X-ray diffraction spectra of the alloy G30 treated at 700°C, 800°C, 900°C and 1000° C after overaging are similar.

The structure of the alloy treated at different temperatures remains monophasic. The appearance of peak at position (a) in diffractogram of the piece treated at 1000°C with a lower intensity compared to the one appeared at 800°C is almost at the same position $2\theta \simeq 27{,}52°$. The same remark for the others temperatures, the positions (b), (c) and (d) correspond to peaks consisting of doublets relative to nickel-based alloy and carbides.

## 4. THE KINETIC STUDY OF THE TRANSFORMATION OF THE ALLOY G30 DURING THE OVER-AGING:

*4.1.APPLICATION OF EQUATION MEHL AND JOHNSON:*

We studied the kinetics of the softening transformation that characterizes the over-aging of the alloy G30 based on hardness measurements. We used the equation of Johnson-Mehl-Avrami [10] in order to determine Avrami index n and constant of rate K. Heat treatments were performed at temperatures 700°C, 800°C,900°C and 1000 °C for 3 hours and the evolution of the evolution of hardness was for a period of 125 days.

The degree of advancement x is calculated from the following relation:

$$X = \frac{HRF(t) - HRF(0)}{HRF(\infty) - HRF(0)}$$

with: $HRF(t)$ = Hardness at time t; $HRF(0)$ = Maximum hardness; $HRF(\infty)$ = Final hardness.

To determine the constants n and k, we plotted Log (-log (1-X)) versus log (t) (figure 23). The linear regression of data points obtained gives a straight line of slope n and x-ordinate log (K). The table 2 gives the values of the exponent n and constant of rate k for the different temperatures.

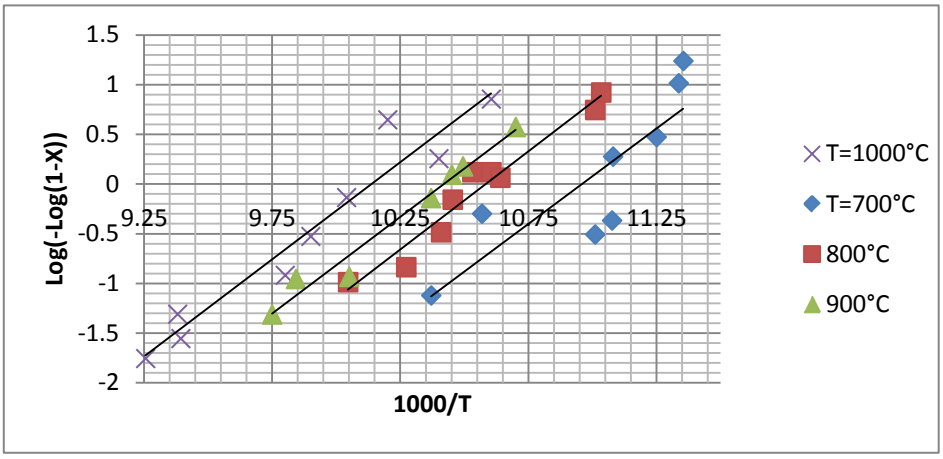


**Figure 23. Log $(-\log(1-X))$ versus $1000/T$ of overaging of the alloy G30 treated at 700 °C, 800 °C, 900 °C and 1000 °C**

**Table 2. The coefficients during overaging of the alloy G30 treated at 700 ° C, 800 ° C, 900° C and 1000 ° C for 3 hours and quenched with water**

| T (°C) | n | K ($min^{-1}$) |
|---|---|---|
| 700 | 1,9165 | 1,73909E-05 |
| 800 | 1,9752 | 2,53245E-05 |
| 900 | 1,9800 | 3,02181E-05 |
| 1000 | 1,9554 | 3,95447E-05 |

We can deduce that the local rearrangement of the atomic structure of the material under thermal action are of the second order (the value of the Avrami index is equal to 1.9) for the four temperatures 700 ° C, 800 ° C, 900 ° C and 1000 ° C.

*4.2. DETERMINATION OF THE APPARENT ACTIVATION ENERGY*

For the determination of activation energy Q, we used the method of Bruke [10]. This method consist on tracing; for a each degree of advancement X; log (t) versus 1/T - as figure 24 shows- which gives a straight line of slope equal to Q / R with R is the constant of ideal gas equal to 8.32 J. $mol^{-1}.s^{-1}$.

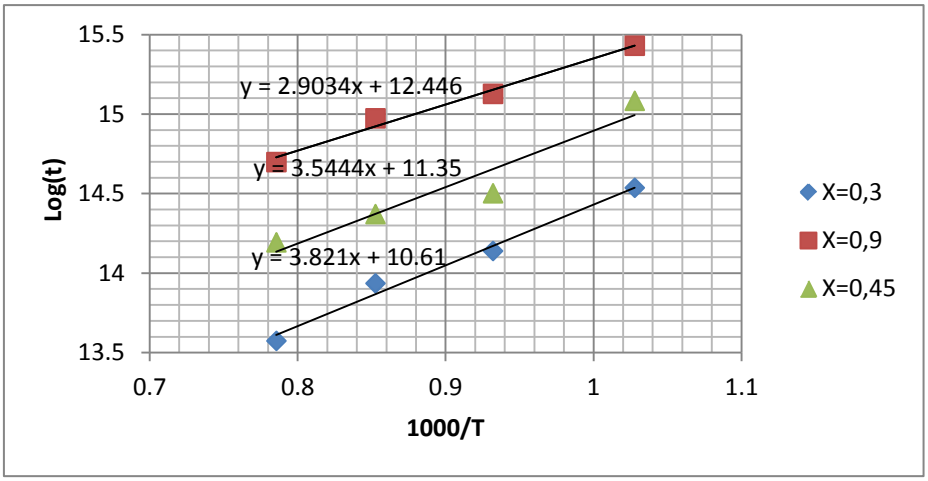


**Figure 24. ln (t) versus $1000/T$ of overaging of the alloy G30 treated at 700 ° C, 800 ° C, 900 ° C and 1000 ° C for 3 hours and then quenched with water.**

The average of the activation energy found for X = 0.3, X = 0.45 and X = 0.9 is equal to 28.47 KJ. $Mol^{-1}$. To verify the results obtained by different laws, we will use the K values determined by Johnson-Mehl-Avrami equation to calculate Q based on Arrhenius relation [11]. The following equation links two constants reaction rate at two different temperatures:

$$\mathrm{Log}\left(\frac{K_1}{K_2}\right) = -\frac{Q}{R} \times \left(\frac{1}{T_1} - \frac{1}{T_2}\right)$$

We found a rate of $\mathbf{28.20\ Kj.mol^{-1}}$, a value close to that determined by the Bruke method.

## 5. CONCLUSIONS

In this work, we treated for 3 hours the nickel-based alloy G30 at 4 different temperatures 700 °C, 800 °C, 900 °C and 1000 °C. The heat treatments performed don't have a large influence on the final mechanical properties of the alloy G30, the hardness of the alloy treated at 700 ° C and 800 ° C is 46 HRF and for those treated at 900 °C and 1000 °C is 46.25 HRF. The nickel-based alloy is developed primarily in order to resist to corrosion at high temperature in corrosive environments. Nevertheless, the iso-thermal treatment led to an inter and intra granular precipitation of chromium carbides in several morphologies and near zones of the latter are poor chromium which makes them likely to be corroded because its anticorrosive power is done by creating on the surface a layer of chromium oxide. The precipitation mechanism is done with the same manner for different temperatures: Formation of precipitates, its decomposition into secondary precipitates and coalescence to form larger areas. The X-ray diffraction spectra obtained after the treatment revealed that the structure remains austenitic, detected the presence of peaks of precipitates for different temperatures and detected also the appearance of a new peak for samples treated at 1000 ° C and 800 ° C. According to JOHNSON-MEHL-Avrami equation, the micro structural transformations are done with a global kinetic almost of order 2 and requires an average of activation energy determined by the method of Bruke and the relation of Arrhenius of 28,335Kj/mol.

## REFERENCES

[1] Meetham, G.W., Van de Voorde, M.H., *The Engineering Materials for High Temperature Engineering Applications*, Springer-Verlag Berlin Heidelberg, 2000.
[2] Winston Revie, R., *Uhlig's Corrosion Handbook*, 3rd Edition, John Wiley & Sons, Inc, Canada, 2004.
[3] ASM International Handbook Committee, *Nickel, Cobalt and Their Alloys*, ASM International, United States of America, 2000.
[4] Totten, G.E. et all, *Handbook of Mechanical Alloy Design*, CRC Press, USA, 2003.
[5] Davids, J.R., *Corrosion: Understanding the Basics*, ASM international, USA, 2000.
[6] ASM International Handbook Committee, *ASM Handbook: Volume 3: Alloy Phase Diagrams*, USA, 1992.
[7] ASM International Handbook Committee, *ASM Handbook: Volume 9: Metallography and Microstructures*, USA, 2004.
[8] Golaski, G., Wieczorek, P., *Archives of Foundry Engineering*, **9**, 97, 2009.
[9] Gharehbaghi, A., *Precipitation Study in A High Temperature Austenitic Stainless Steel Using Low Voltage Energy Dispersive X-Ray Spectroscopy*, Master Degree Project, University Royal Institute of Technology, 2012.
[10] Bruke, J., *The kinetics of phases transformations in metals*, Pergamon Press, New York, 1965.
[11] Saissi, S. et all, *Journal of Science and Arts*, **4**(29), 331, 2014.